Selective Production of Hydrogen Isotope Gases via PdAg-Catalyzed Dehydrogenation of Formic Acid in D_2O Assisted by Surface-grafted Amine Groups

Kohsuke Mori[a,b]*, Atsushi Konishi[a], Tatsuya Fujita[a], and Hiromi Yamashita[a,b]

[a] Division of Materials and Manufacturing Science, Graduate School of Engineering, Osaka University, 2-1 Yamada-oka, Suita, Osaka 565-0871, Japan.

Tel: +81-6-6879-7460, E-mail: mori@mat.eng.osaka-u.ac.jp

[b] Innovative Catalysis Science Division, Institute for Open and Transdisciplinary Research Initiatives (ICS-OTRI), Osaka University

Abstract

Hydrogen isotope gases are widely used as deuterium sources in industrial manufacturing processes. It would therefore be beneficial to develop a facile, simple means of selective producing molecular deuterium (D_2) and hydrogen deuteride (HD), although reasonable heterogeneous catalytic methodologies are still missing. We previously demonstrated that the hydrogen isotope gases was selectively obtained from formic acid (HCOOH, FA) and D_2O using PdAg nanoparticles supported on mesoporous silica (SBA-15) on which amine functional groups had been grafted. In the present work, amine-functionalized carbon was used as an efficient support material to provide a catalyst with improved activity. Employing weakly basic phenylamine groups, D_2 was predominantly evolved and the reaction rate was doubled compared with that for our previously reported system. A high degree of correlation between D_2 selectivity and the basicity of the grafted amine groups was also observed. The applicability of the present catalytic system was highlighted by *in situ* deuteration of diphenylacetylene in a solution of FA in D_2O, during which deuterated products were obtained with high efficiency.

Keywords: hydrogen isotope gas, formic acid, alloy nanoparticles, amine modification

Highlights

- Hydrogen isotope gases were produced from formic acid and D_2O in a controlled manner
- PdAg nanoparticles and grafted amine groups acted cooperatively to selectively generate hydrogen isotope gases
- D_2 selectivity was highly correlated with basicity of the amine moiety on support
- This system allowed the *in situ* deuteration of diphenylacetylene

Graphic abstract

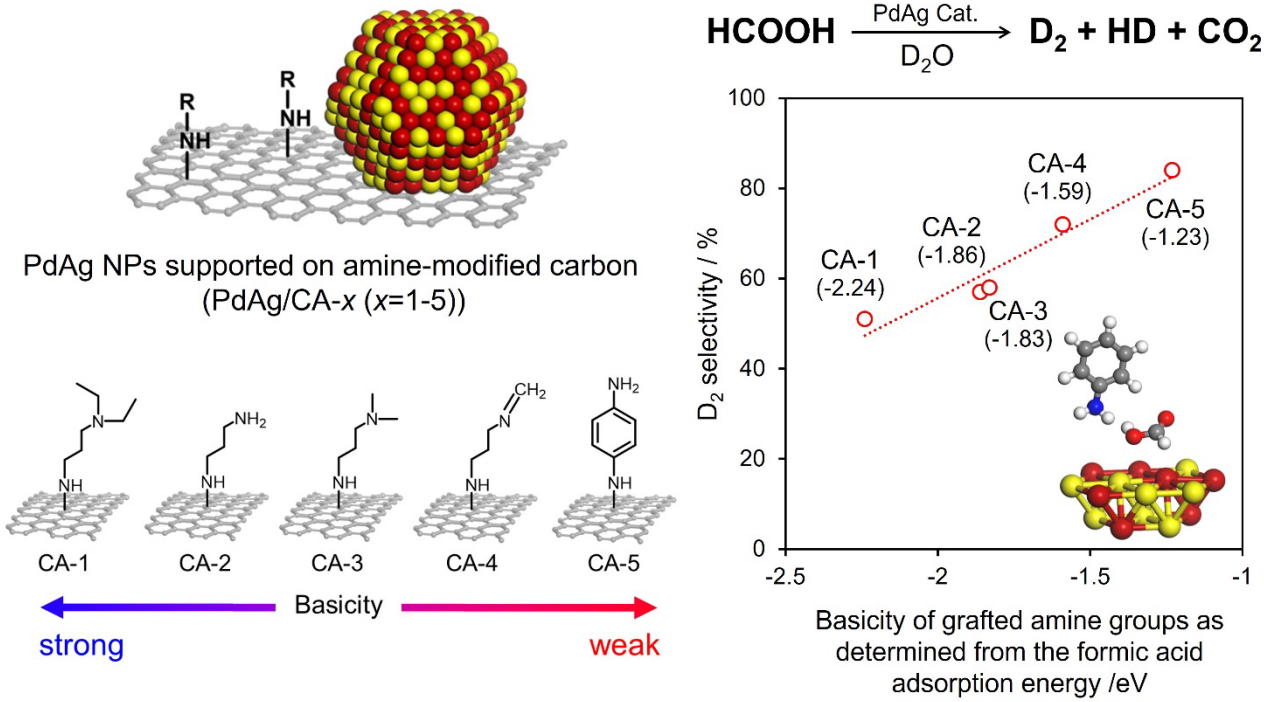

1. Introduction

The establishment of reliable techniques for hydrogen storage and transportation is expected to achieve a future hydrogen society.[1, 2] In this respect, liquid organic hydrogen carriers are regarded as feasible alternatives to the conventional physical hydrogen storage.[3-5] Among them, formic acid (HCOOH, FA) has received considerable attention. This compound exhibits low toxicity, is a nonflammable and has a high hydrogen content (52 g H_2 L^{-1}).[6-8] The employment of FA as a possible liquid hydrogen carriers could therefore enable reasonable carbon dioxide (CO_2)-mediated hydrogen storage energy cycle through the CO_2 hydrogenation with H_2 to regenerate FA.[9-12] Considerable progress has been made for discovering both homogeneous and heterogeneous metal catalysts, which are capable of facilitating H_2 release from FA.[13-18] The selective release of H_2 from FA is thermodynamically favored (HCOOH → H_2 + CO_2, $\Delta G = -48.4$ kJ·mol^{-1}), which is crucial for the generation of pure H_2 suppressing undesired dehydration reaction (HCOOH → H_2O + CO, $\Delta G = -28.5$ kJ·mol^{-1}), because the formation of CO contamination poisons the catalyst.

H_2 is a highly important next-generation energy source. However, gaseous molecular deuterium (D_2) and hydrogen deuteride (HD) are also expensive specialty gases used as reagents for a wide variety of research purposes.[19] Currently, D_2 is typically produced by the electrolysis of D_2O, which requires a large amount of energy, while HD is synthesized by catalytic isotope exchange between H_2 and D_2, with a maximum theoretical yield of 50%. Thus, a simple catalytic process for the synthesis of these compounds would be highly desirable. A number of metal-catalyzed H/D exchange reactions between H_2 and D_2O have been developed using homogenous metal complex catalysts.[20-22] The heterogenous Pd/C-catalyzed D_2 generation from a H_2-D_2O combination was also investigated by Sajiki et al.[23] More recently, Fujita et al., developed a catalytic method to produce D_2 from CD_3OD using Ir complex.[24] Interestingly, the generation of hydrogen isotope gases via H-D exchange reactions in association with the dehydrogenation of FA in D_2O using transition metal complexes such as Ru, Rh and Ir.[25-28] Although some progress has been achieved, high catalyst concentrations are often required along with expensive deuterated FA analogues, such as HCOOD, DCOOH or DCOOD. Furthermore, the industrial utilization of homogeneous metal complexes is severely limited owing to the complications in recycling of the expensive catalyst metals and ligands.

We have previously reported a simple protocol for the release of hydrogen isotope gases from only pure FA together with D_2O as a solvent using PdAg nanoparticles (NPs) supported on amine

functionalized mesoporous silica SBA-15.[29] Interestingly, the selectivity can be controlled by changing the amine groups with different basicity. Upon consideration of the experimental data and of theoretical investigation, a probable reaction pathway for the selective formation of hydrogen isotope gases is proposed, as illustrated in **Figure 1**. This process is initiated by the O−H bond dissociation of an FA molecule on a NP (**I**) with the assistance of an adjacent amine group to generate a metal-formate intermediate with a protonated amine group (**II**).[30, 31] Subsequently, the Pd-formate species undergoes hydride elimination to generate a Pd hydride and release CO_2 (**III**). Following the addition of D_2O to the catalyst in this state, a H-D exchange reaction occurs involving both the Pd hydride and the basic amine site, as in (**IV)** or (**VII)**. The possible subsequent reactions will proceed to different extents depending on the interaction with grafted basic amine moiety. In the presence of strongly basic $-NEt_2$ groups (**IV**), H-D exchange preferentially occurs at the Pd site leading to the scenario (**V**) rather than at the basic amine site leading to (**VI**). Because the energy barrier for the formation of intermediate (**VI)** is much higher than that for (**V)**, HD is preferentially generated. In contrast, the activation energy values on going from (**VII)** to form (**VIII)** and (**IX)** are comparable. This allows reactions to proceed at both sites, resulting in the predominant formation of (**IX)** such that D_2 production is favored. Conclusively, the specific hydrogen isotope gas selectivity is governed by the extent to which the H-D exchange reaction takes place at basic sites around the active centers.

In the course of our ongoing studies exploring more practical heterogeneously-catalyzed systems, the work reported herein determined that amine-functionalized carbon provides an efficient support material for this targeted reaction that exhibits improved activity. This work also confirms that the preferential formation of specific hydrogen isotope gases can be tuned by changing the amine moieties with different basicity. Other interesting aspects, including the applications to the *in situ* deuteration of diphenylacetylene in an FA/D_2O solution are also examined.

2. Experimental Section

2.1. Chemicals: $AgNO_3$, *p*-phenylenediamine, sodium borohydride ($NaBH_4$), formic acid (FA) and sodium formate (SF) were obtained from Nakalai Tesque, Inc. $Pd(NH_3)_4Cl_2$ was purchased from the

Aldrich Chemical Co. Carbon support (Ketjen Black, EC600JD) was obtained from LION Speciality Chemicals Co., LTD.

2.2. Synthesis of amine functionalized carbon supports (CA-*x*)[32]**:** The carbon support (100 mg) was added into 50 mL of HNO_3 solution (60 %) and heated at 353 K. After 5h, the resulting suspension was filtered and washed thoroughly with distilled water until the pH of filtrate reaches 7. Next, the obtained acid treated carbon (CA, 1.0 g) was combined with 50 mL of acetone containing *p*-phenylenediamine (3.24 g) and stirred at RT for two days. After the filtration and washing with acetone and distilled water for several times, giving CA-5. The use of other amines instead of *p*-phenylenediamine, such as N,N-diethyl-1,3-diaminopropane, 1,3-diaminopropane, N,N-dimethyl-1,3-diaminopropane, gave CA-1, CA-2, and CA-3, respectively. The CA-4 including Schiff base group (-N=CH_2) was obtained by the additional treatment of CA-2 specimen with an aqueous formaldehyde (HCHO) solution.

2.3. Synthesis of PdAg/amine functionalized carbon (PdAg/CA-*x*): CA-x (300 mg) was dispersed in 50 mL of an aqueous metal precursor solution that contained both $Pd(NH_3)_4Cl_2$ (0.01 M, 2.85 mL) and $AgNO_3$ (0.01 M, 2.85 mL), and stirred at R.T. After 1 h, the injection of $NaBH_4$ aqueous solution into the above solution, affording PdAg/CA-*x* (1 wt% Pd; molar ratio of Pd:Ag = 1:1).

2.4. Characterization: N_2 adsorption-desorption isotherms, Brunauer–Emmett–Teller surface areas (S_{BET}), high-angle annular dark-field scanning transmission electron microscopy (HAADF-STEM) images and energy-dispersive X-ray (EDX) elemental mapping, XPS spectra, and X-ray absorption fine structure (XAFS) spectra at Pd and Ag K-edge were acquired according to procedures described previously.[29] Analysis of XAFS data was conducted using the Rigaku REX2000.

2.5. Catalytic FA dehydrogenation: The catalyst (50 mg) was placed into a reaction vessel containing D_2O (2.6 mL). After the addition of 5M FA:SF (9:1) in D_2O (0.2 mL), the resulting mixture was subsequently reacted at 343 K under an Ar atmosphere. The analysis of hydrogen isotope gases (i.e. H_2, HD and D_2) were conducted by Shimadzu GC–2014 (He carrier) equipped with a TCD using a Shinwa OGO–SP columns at 77 K [33] Turnover frequency (TOF, h^{-1}) values were defied as (mol

of all hydrogen isotope gases)/(mol of Pd). After the first reaction, catalyst was filtered and dried under vacuum. The second reaction was carried out using 50 mg of spent catalyst, which is combining the two sets of first reactions.

2.6. *In situ* deuteration of diphenylacetylene: PdAg/CA-5 (50 mg), D_2O (4.8 mL), and diphenylacetylene (0.1 mmol) were placed into a reaction vessel. After the addition of 5M FA:SF (9:1) in D_2O (0.2 mL), the resulting mixture was subsequently reacted at 353 K under an Ar atmosphere. After the reaction, the aqueous filtrate was extracted with Et_2O, dried over $MgSO_4$, and obtained analytically pure deuterated produces by the concentration in vacuo. The product was analyzed by ^1H NMR spectroscopy and the product distribution was determined by GC-MS.

2.7. Calculation of the adsorption energy of FA: Density Functional Theory (DFT) calculations under periodic boundary conditions was conducted with the DMol^3 program in the Materials Studio 17.2 interface.[34] The GGA exchange-correlation functional proposed by PBE was combined with the DNP functions. The experimentally prepared PdAg alloy NPs were modeled as a supercell slab consisting of a 4 × 4 surface unit cell with three atomic (111) surface layers, in which Pd and Ag atoms are alternately arranged. The top layer was allowed to relax, while the bottom two layers were fixed in the geometry optimization process. The slab models have a vacuum space with a thickness of 30 Å. E_{ad} is defined as $E_{ad} = E_{FA/slab} - (E_{FA} + E_{slab})$, where $E_{FA/slab}$, $E_{FA,}$ and E_{slab} and are the total energies of the FA/slab system, free FA, and bare slab, respectively.

3. Results and Discussion

3.1. Synthesis and characterization of catalyst

A series of amine-grafted carbon supports (denoted herein as CA-*x*, where *x* = 1-5) were fabricated by the surface modification procedure. The synthetic procedure is shown in **Figure 2**. In this process, the carbon support was immersed with an aqueous HNO_3 solution to produce various surface oxygen-based functional groups (e.g. –COOH, –OH, and C–O–C). Temperature programed desorption (TPD) experiments under He flow conditions showed the peak of CO_2 (m/z=44) at around 350 ºC, which is

ascribed to carboxyl group (-COOH), and the peak of the CO (m/z=28) at around 500 ºC and 750 ºC, which are attributed to hydroxyl (-OH) and ether (C-O-C) groups, respectively (**Figure S1**).[35] In a typical reaction, these groups were subsequently reacted with *p*-phenylenediamine to afford amide and C–N bonds, affording CA-5. The use of other amines having different basicity values, including N,N-diethyl-1,3-diaminopropane, 1,3-diaminopropane and N,N-dimethyl-1,3-diaminopropane gave CA-1, CA-2 and CA-3, respectively. The CA-4 involving Schiff base functional group (-N=CH_2), was produced by the modification of CA-2 by reaction with aqueous formaldehyde. These supports were subsequently immersed in precursor solutions of Pd and Ag, and then conducted a chemical reduction with aqueous $NaBH_4$ solution. The obtained specimens are represented as PdAg/CA-*x* (*x* = 1-5). The amount of N content in each material was estimated to be approximately 0.6 mmol·g^{-1} by CHN elemental analysis, as summarized in **Table S1**, which accompanied with the surface amine contents. The S_{BET} and pore volumes (V_p) for the specimens obtained from the N_2 adsorption/desorption are shown in **Figure S2** and **Table S2**. The S_{BET} and V_p of original unmodified carbon were 1487 $m^2 \cdot g^{-1}$ and 3.9 $cm^3 \cdot g^{-1}$. The acid treatment slightly decreased (S_{BET} = 1203 $m^2 \cdot g^{-1}$, V_p = 2.9 $cm^3 \cdot g^{-1}$), while the subsequent amine functionalization significantly declined (S_{BET} = 479 $m^2 \cdot g^{-1}$, V_p = 2.0 $cm^3 \cdot g^{-1}$). The deposition of the catalyst metals resulted in further decrease (S_{BET} = 407 $m^2 \cdot g^{-1}$, V_p = 1.9 $cm^3 \cdot g^{-1}$). The functionalization with other amine groups also provides similar results (**Figure S3** and **Table S3**). The monometallic Pd/CA-5 without the alloying by Ag and the PdAg/C without the amine modification were also synthesized by similar method.

A HAADF-STEM image of the PdAg/CA-5 are shown in **Figure 3a**. The generated PdAg NPs were apparently well distributed with a narrow size distribution, in which a mean particle size was determined to be 5.6 nm. The EDX mapping of a selected area shown in this figure also demonstrate that the N atoms were highly dispersed on the support material and that the white particles seen in the image were composed of Pd and Ag (**Figure 3b-e**). The STEM images of the other PdAg/CA-*x* (*x* = 1-4) specimens also indicated good dispersion of the PdAg NPs and that these NPs had average diameters of 4.5-6.5 nm (**Figure S4**). These results confirm that variations of the grafted amine groups with different basicity induced the different interaction with precursors, which affected not only the initial generation of the Pd nuclei but also the successive growth of these NPs with varied sizes.

The shapes of X-ray absorption near edge structure (XANES) spectra of the prepared PdAg/CA-1 and PdAg/CA-5 at the Pd K-edge differed from that obtained from metallic Pd foil but resembled

that for PdO (**Figure 4A**). The extended X-ray absorption fine structure (EXAFS) spectra of both specimens displayed two distinct peaks due to the Pd−O(N) bonds in the vicinity of 1.6 Å and Pd−Pd bonds at around 2.7 Å (**Figure 4B**). The contiguous Pd−Pd bond distance in these specimens were also found to be slightly larger than those in Pd foil, confirming that Pd−Ag bonds with longer distances were present. The peak at shorter distance is considered to be partly due to Pd–N contribution, which is originated from the interactions with the surface amine groups.[32] The XANES spectra of the PdAg/CA-1 and PdAg/CA-5 at Ag K-edge were resemble to that for the reference Ag foil (**Figure 4C**). In addition, the Ag K-edge EXAFS spectra of our prepared specimens exhibited a single peak attributed to the Ag−Ag bond centered at around 2.7 Å (**Figure 4D**). The slight shift toward a shorter distance compared to that for reference Ag metal indicates the existence of Pd−Ag bonds with longer interatomic distances. Furthermore, the Pd 3d peaks of the PdAg/CA-1 and PdAg/CA-5 were shifted to higher binding energies in comparison to that of PdAg/C without amine functionalization, and a similar tendency was observed in the case of the Ag 3d peaks (**Figure S5**). These results confirmed that the surface amine groups in the vicinity of the supported PdAg NPs altered their electronic states.

3.2. Selective production of hydrogen isotope gases

The time courses for the gas evolution during the dehydrogenation of FA in D_2O solutions containing FA:SF (9:1) at 343 K are plotted in **Figure 5A**. In addition, the selectivities for H_2, HD and D_2 are summarized in **Figure 5B**. The ratio of the total moles of hydrogen isotope gases to moles of CO_2 was constantly almost 1 for each sample. Note that the undesirable CO formation reaction can be suppressed to < 2 ppm (the detection limit of the GC). The PdAg/CA-5, which has weakly basic –$PhNH_2$ groups, displayed the highest activity along with the preferential generation of D_2 with 84% selectivity. D_2 selectivity increased with increasing the amount of D_2O solvent, accompanied with the decrease of TOF (**Figure S6**). The catalytic activity shown by the monometallic Pd/CA-5 was low. This outcome established that alloying with Ag showed the promotional effect in the C–H bond dissociation step occurring during the dehydrogenation of FA, as discussed previously.[30, 36] The use of PdAg/C gave lower activity and reduced D_2 selectivity (66%), providing further evidence for the importance of the surface amine groups in terms of promoting the O–H bond dissociation step and in determining selectivity. The catalytic activity of PdAg/CA-5 was more than twice that obtained

for the PdAg/SA-5 catalyst (d_{ave} = 4.5 nm, S_{BET} = 635 $m^2 \cdot g^{-1}$, V_p = 1.2 $cm^3 \cdot g^{-1}$) employed in our previous work. The latter material was prepared by surface modification of mesoporous silica (SBA-15) substrates with aminophenyltrimethoxysilane.[29] Moreover, the unsupported PdAg NPs, prepared by the $NaBH_4$ chemical reduction of metal precursors in the presence of PVP, showed almost no activity because of the aggregation into larger particles under the catalytic reaction conditions.

In the preliminary experiments, the use of Ketjen Black provided better activity compared with other carbon supports, such as Shirasagi and Vulcan X. The activated carbon Shirasagi has larger size distribution of particles and possesses microporous structure. The particle size of Vulcan X is uniform, but the specific surface area is not high enough (S_{BET} =270 m^2/g) because of the lack of porosity. On the contrary, Ketjen black possesses both mesoporous channel and uniform microporous structure, which presumably allows the efficient adsorption of reactants.[37]

The influence of the different amine groups on the selectivities for the resulting hydrogen isotope gases are examined, as shown in **Figure 5C**, along with the TOF (h^{-1}) based on the Pd employed. The selectivity could evidently be altered by changing the type of amine; the PdAg/CA-1, which was modified with strongly basic $-NEt_2$ groups, showed 51% D_2 selectivity, while 87% selectivity was observed when using PdAg/CA-5 having weakly basic $-PhNH_2$ groups. The hydrogen isotope gases can be generated with high reproducibility; the standard deviations of D_2 selectivity are 1.70, 0.81, 1.53, 1.01, 1.29, and 1.34 for PdAg/CA-*x* (*x*=0-5), respectively. The TOF was also affected by the kind of the amine functional groups such that the TOF attained with PdAg/CA-5 was 688 h^{-1}, in which amine surface contents rather than basicity is a crucial factor, as discussed later. This value was higher than that attained with PdAg/CA-4 by a factor of 3. It should be noted that the attained high D_2 selectivity is higher or comparable than those obtained via the dehydrogenation of FA in D_2O using transition metal complexes such as Ru, Rh and Ir, although they employed expensive deuterated FA analogues, such as HCOOD, DCOOH or DCOOD, as summarized in **Table S4.** [25-27]

To better understand the differences in selectivity, the FA adsorption energy (E_{ad}) was determined based on density functional theory calculations for each material. This parameter was used because the adsorption energy reflected the basicity of the amine group owing to the formation of a FA–amine complex via hydrogen bonding.[31] The E_{ad} over CA-1 (having $-NEt_2$ groups) was -2.24 eV and so was significantly higher than the value of -1.23 eV for CA-5 (with $-PhNH_2$ groups). Interestingly, we

found a good relationship between the selective D_2 evolution and E_{ad}, in which the D_2 preferentially obtained with increasing E_{ad} (**Figure 5D**). On the contrary, no evident correlation was observed between the selectivity and the mean size of PdAg NP as estimated by HAADF-STEM analyses (**Figure S7**). Furthermore, the D_2 selectivity was found to be approximately 90% independent of the quantity of phenylamine groups grafted onto PdAg/CA-5, although the TOF increased with increasing amount (**Figure 5E**). These results evidenced that the basicity of the amine moieties on the periphery of the active centers played an important role in determining the selectivity as opposed to the intrinsic catalytic ability of the metal NPs. In a separate experiment, PdAg/CA-5 was simply isolated from the reaction medium and the spent catalyst could be reused while keeping its activity and preferential D_2 selectivity (**Figure 5F**). Thus, the amine groups appear to have been thermally and mechanically stable on the carbon support, which would also be expected to stabilize the PdAg NPs. On the contrary, a physical mixture of PdAg/C and *p*-phenylenediamine showed minimal activity, and the performance of this material was further decreased during a second usage after the recovery of the powdered catalyst from the reaction medium.

The ability to perform the subsequent chemical reactions in the same reaction vessel is a promising approach to sustainable chemistry and the lacking of isolation steps of intermediates can reduce time and energy expenditures as well as waste production.[24, 27, 38, 39] To assess this possibility, the present catalytic system was applied to the simple and efficient *in situ* deuteration of diphenylacetylene. The reaction proceeded smoothly in the presence of PdAg/CA-5 and D_2O solution containing FA:SF (9:1) for 6h, where the product with 95% D content was obtained in 99% chemical yield, as confirmed by ^{1}H NMR (**Figure S8**). This activity is higher than that attained with our previously reported PdAg/SA-5, which was prepared by the amine modification of SBA-15, in which the deuterated product was obtained with 79% D content for 6h. The activation energy (E_a) for the deuteration of diphenylacetylene using PdAg/CA-5 and D_2O-FA determined from Arrhenius plots, was 35.6 kJ mol^{-1}, as shown in **Figure S9**. This value is larger than 26.9 kJ mol^{-1} for hydrogenation of diphenylacetylene using PdAg/CA-5 and H_2O-FA, indicating D_2O acts not only as solvent, but also as reagents for the deuteration.

Next, the effect of deuterium source was investigated. **Figure 6A** shows the possible deuterated compounds and their corresponding molecular weights (MWs). The product distributions obtained from these trials were using the intensity of fragment ion peak based on m/z determined by GC-mass

spectrometry (MS), as provided in **Figure 6B**. The deuteration reaction of diphenylacetylene by PdAg/CA-5 in the combination of FA-D_2O afforded the distribution of deuterated product with m/z =186 is 60% for 3h. On the contrary, the introduction of gaseous D_2 into an H_2O solution retarded the reaction and exhibited low deuteration efficiency. The specificities for the products with m/z =186 and 182 were 3% and 71%, respectively, after 6 h. The reaction using H_2 gas together with a D_2O solution afforded 54% specificity for the m/z =186 product but required a longer reaction time compared with that needed for the FA/D_2O system. These results indicate that the present FA-D_2O system is the metal-catalyzed transfer hydrogenation and the mechanism involving the in situ generated H_2 gas from FA decomposition are minor pathway. Moreover, one possible reason for the high activity exhibited by the FA/D_2O system is the two-phase nature of this process, comprising a solid catalyst together with liquid FA and D_2O. This scenario likely facilitated the H-D exchange reaction compared with three-phase systems including a solid catalyst, liquid H_2O or D_2O and gaseous H_2 or D_2.

4. Conclusion

This work demonstrated the selective generation of hydrogen isotope gases via FA dehydrogenation in D_2O by adjusting the grafted amine groups. This was accomplished based on the cooperative action on a PdAg nanocatalyst dispersed over an amine-functionalized carbon-based support. The amine groups grafted onto the support were found to be crucial and the selectivity was determined to vary with the basicity of these groups. Specifically, the selectivity for D_2 increased with decreasing basicity. The *in situ* deuteration of diphenylacetylene using PdAg/SA-5 together with FA and D_2O proceeded smoothly, giving a highly deuterated product in excellent chemical yield. This study provides important insights into the catalyst design and further reveals a promising heterogeneous catalyst system for this particular chemical reaction. Further application of the present catalytic system is now under investigation.

Author contributions

K.M. conceived the idea, designed the experiments, carried out DFT calculations and wrote the manuscript. A.K. performed the sample preparation, characterization, and catalytic test. T.F. helped the catalyst characterization. H.Y. helped supervise the project.

Declaration of competing interest

The authors declare no competing financial interest.

Data availability

Data will be made available on request.

Acknowledgement

This work has been supported by A21H50980 and T22K189200 from the Japan Society for the Promotion of Science (JSPS). K.M. also acknowledge the TOYOTA Mobility foundation (TMF) and the Iwatani Naoji Foundation. The XAFS experiments were performed at the beamline 01B1 station at SPring-8 with the approval from JASRI (2020A1062 and 2021A1095). TEM experiment was partly conducted using a facility in the Research Center for Ultra-High Voltage Electron Microscopy at Osaka University.

Appendix A. Supplementary data

Supplementary data to this article can be found online

References

[1] M. Otto, K.L. Chagoya, R.G. Blair, S.M. Hick, J.S. Kapat, Optimal hydrogen carrier: Holistic evaluation of hydrogen storage and transportation concepts for power generation, aviation, and transportation, J. Energy Storage, 55 (2022) 105714. https://www.sciencedirect.com/science/article/pii/S2352152X22017029

[2] O. Faye, J. Szpunar, U. Eduok, A critical review on the current technologies for the generation, storage, and transportation of hydrogen, Int. J. Hydrogen Energy, 47 (2022) 13771-13802. https://www.sciencedirect.com/science/article/pii/S0360319922007261

[3] M.R. Usman, Hydrogen storage methods: Review and current status, Renewable Sus. Energy Rev., 167 (2022) 112743. https://www.sciencedirect.com/science/article/pii/S1364032122006311

[4] V. Yadav, G. Sivakumar, V. Gupta, E. Balaraman, Recent advances in liquid organic hydrogen carriers: an

alcohol-based hydrogen economy, ACS Catal., 11 (2021) 14712-14726. https://doi.org/10.1021/acscatal.1c03283

[5] H. Jeong, T.W. Kim, M. Kim, G.B. Han, B. Jeong, Y.-W. Suh, Mesoporous acidic SiO_2–Al_2O_3 support boosts nickel hydrogenation catalysis for H_2 storage in aromatic lohc compounds, ACS Sus. Chem. Eng., 10 (2022) 15550-15563. https://doi.org/10.1021/acssuschemeng.2c04978

[6] A.K. Singh, S. Singh, A. Kumar, Hydrogen energy future with formic acid: a renewable chemical hydrogen storage system, Catal. Sci. Tech., 6 (2016) 12-40. http://dx.doi.org/10.1039/C5CY01276G

[7] D. Mellmann, P. Sponholz, H. Junge, M. Beller, Formic acid as a hydrogen storage material - development of homogeneous catalysts for selective hydrogen release, Chem. Soc. Rev., 45 (2016) 3954-3988. http://dx.doi.org/10.1039/C5CS00618J

[8] S. Zhai, S. Jiang, C. Liu, Z. Li, T. Yu, L. Sun, G. Ren, W. Deng, Liquid Sunshine: Formic Acid, J. Phys. Chem. Lett., 13 (2022) 8586-8600. https://doi.org/10.1021/acs.jpclett.2c02149

[9] D.A. Bulushev, J.R.H. Ross, Heterogeneous catalysts for hydrogenation of CO_2 and bicarbonates to formic acid and formates, Catal. Rev., 60 (2018) 566-593. https://doi.org/10.1080/01614940.2018.1476806

[10] G.H. Gunasekar, K. Park, K.-D. Jung, S. Yoon, Recent developments in the catalytic hydrogenation of CO_2 to formic acid/formate using heterogeneous catalysts, Inorg. Chem. Front., 3 (2016) 882-895. http://dx.doi.org/10.1039/C5QI00231A

[11] K. Mori, T. Sano, H. Kobayashi, H. Yamashita, Surface engineering of a supported PdAg catalyst for hydrogenation of CO_2 to formic acid: Elucidating the active Pd atoms in alloy nanoparticles, J. Am. Chem. Soc., 140 (2018) 8902-8909. https://doi.org/10.1021/jacs.8b04852

[12] K. Mori, H. Hata, H. Yamashita, Interplay of Pd ensemble sites induced by GaO_x modification in boosting CO_2 hydrogenation to formic acid, Appl. Catal. B: Environ., 320 (2023) 122022. https://doi.org/10.1016/j.apcatb.2022.122022

[13] N. Wang, Q. Sun, R. Bai, X. Li, G. Guo, J. Yu, In situ confinement of ultrasmall pd clusters within nanosized silicalite-1 zeolite for highly efficient catalysis of hydrogen generation, J. Am. Chem. Soc., 138 (2016) 7484-7487. https://doi.org/10.1021/jacs.6b03518

[14] J. Eppinger, K.-W. Huang, Formic Acid As A Hydrogen Energy Carrier, ACS Energy Lett., 2 (2017) 188-195. https://doi.org/10.1021/acsenergylett.6b00574

[15] E. Doustkhah, M. Hasani, Y. Ide, M.H.N. Assadi, Pd nanoalloys for H_2 generation from formic acid, ACS Appl. Nano Mater., 3 (2020) 22-43. https://doi.org/10.1021/acsanm.9b02004

[16] M. Younas, M. Rezakazemi, M.S. Arbab, J. Shah, W.U. Rehman, Green hydrogen storage and delivery: Utilizing highly active homogeneous and heterogeneous catalysts for formic acid dehydrogenation, Inter. J. Hydrogen Energy, 47 (2022) 11694-11724. https://www.sciencedirect.com/science/article/pii/S0360319922003561

[17] W.-Y. Yu, G.M. Mullen, D.W. Flaherty, C.B. Mullins, Selective hydrogen production from formic acid decomposition on Pd–Au bimetallic surfaces, J. Am. Chem. Soc., 136 (2014) 11070-11078. https://doi.org/10.1021/ja505192v

[18] Y. Minami, Y. Amao, Catalytic mechanism for selective hydrogen production based on formate decomposition with polyvinylpyrrolidone-dispersed platinum nanoparticles, Sustainable Energy Fuels, 4 (2020) 3458-3466. http://dx.doi.org/10.1039/D0SE00363H

[19] A. Vértes, S. Nagy, Z. Klencsár, R.G. Lovas, Handbook of nuclear chemistry, Kluwer Academic Publishers2003.

[20] A. Azua, S. Sanz, E. Peris, Water-soluble Ir^{III} N-heterocyclic carbene based catalysts for the reduction of CO_2 to formate by transfer hydrogenation and the deuteration of aryl amines in water, Chem. Eur. J., 17 (2011) 3963-3967. https://onlinelibrary.wiley.com/doi/abs/10.1002/chem.201002907

[21] G. Kovács, L. Nádasdi, G. Laurenczy, F. Joó, Aqueous organometallic catalysis. Isotope exchange reactions in H_2–D_2O and D_2–H_2O systems catalyzed by water-soluble Rh- and Ru-phosphine complexes, Green Chem., 5 (2003) 213-217. http://dx.doi.org/10.1039/B300156N

[22] F.A. Jalón, B.R. Manzano, A. Caballero, M.C. Carrión, L. Santos, G. Espino, M. Moreno, Facile Ru−H_2 heterolytic activation and intramolecular proton transfer assisted by basic n-centers in the ligands, J. Am. Chem. Soc., 127 (2005) 15364-15365. https://doi.org/10.1021/ja055116f

[23] T. Kurita, F. Aoki, T. Mizumoto, T. Maejima, H. Esaki, T. Maegawa, Y. Monguchi, H. Sajiki, Facile and convenient method of deuterium gas generation using a Pd/C-catalyzed H_2–D_2 exchange reaction and its application to synthesis of deuterium-labeled compounds, Chem. Eur. J., 14 (2008) 3371-3379. https://onlinelibrary.wiley.com/doi/abs/10.1002/chem.200701245

[24] A. Enomoto, S. Kajita, K.-i. Fujita, Convenient method for the production of deuterium gas catalyzed by an iridium complex and its application to the deuteration of organic compounds, Chem. Lett., 48 (2019) 106-109. https://www.journal.csj.jp/doi/abs/10.1246/cl.180870

[25] S. Fukuzumi, T. Kobayashi, T. Suenobu, Efficient catalytic decomposition of formic acid for the selective generation of H_2 and H/D exchange with a water-soluble rhodium complex in aqueous solution,

ChemSusChem, 1 (2008) 827-834. https://onlinelibrary.wiley.com/doi/abs/10.1002/cssc.200800147

[26] S. Fukuzumi, T. Kobayashi, T. Suenobu, Unusually large tunneling effect on highly efficient generation of hydrogen and hydrogen isotopes in pH-selective decomposition of formic acid catalyzed by a heterodinuclear iridium−ruthenium complex in water, J. Am. Chem. Soc., 132 (2010) 1496-1497. https://doi.org/10.1021/ja910349w

[27] W.-H. Wang, J.F. Hull, J.T. Muckerman, E. Fujita, T. Hirose, Y. Himeda, Highly efficient D_2 generation by dehydrogenation of formic acid in D_2O through H^+/D^+ exchange on an iridium catalyst: Application to the synthesis of deuterated compounds by transfer deuterogenation, Chem. Eur. J., 18 (2012) 9397-9404. https://onlinelibrary.wiley.com/doi/abs/10.1002/chem.201200576

[28] Y. Gao, J.K. Kuncheria, H.A. Jenkins, R.J. Puddephatt, G.P.A. Yap, The interconversion of formic acid and hydrogen/carbon dioxide using a binuclear ruthenium complex catalyst, J. Chem. Soc., Dalton Trans., (2000) 3212-3217. http://dx.doi.org/10.1039/B004234J

[29] K. Mori, Y. Futamura, S. Masuda, H. Kobayashi, H. Yamashita, Controlled release of hydrogen isotope compounds and tunneling effect in the heterogeneously-catalyzed formic acid dehydrogenation, Nat. Commun., 10 (2019) 4094. https://doi.org/10.1038/s41467-019-12018-7

[30] K. Mori, M. Dojo, H. Yamashita, Pd and Pd–Ag nanoparticles within a macroreticular basic resin: An efficient catalyst for hydrogen production from formic acid decomposition, ACS Catal., 3 (2013) 1114-1119. http://dx.doi.org/10.1021/cs400148n

[31] K. Mori, S. Masuda, H. Tanaka, K. Yoshizawa, M. Che, H. Yamashita, Phenylamine-functionalized mesoporous silica supported PdAg nanoparticles: a dual heterogeneous catalyst for formic acid/CO_2-mediated chemical hydrogen delivery/storage, Chem. Commun., 53 (2017) 4677-4680. http://dx.doi.org/10.1039/C7CC00864C

[32] S. Masuda, K. Mori, Y. Futamura, H. Yamashita, PdAg nanoparticles supported on functionalized mesoporous carbon: Promotional effect of surface amine groups in reversible hydrogen delivery/storage mediated by formic acid/CO_2, ACS Catal., 8 (2018) 2277-2285. https://doi.org/10.1021/acscatal.7b04099

[33] S. Ogo, K. Ichikawa, T. Kishima, T. Matsumoto, H. Nakai, K. Kusaka, T. Ohhara, A Functional [NiFe]hydrogenase mimic that catalyzes electron and hydride transfer from H_2, Science, 339 (2013) 682-684. https://science.sciencemag.org/content/sci/339/6120/682.full.pdf

[34] B. Delley, From molecules to solids with the $DMol^3$ approach, J. Chem. Phys., 113 (2000) 7756-7764. https://doi.org/10.1063/1.1316015

[35] H. Nishihara, S. Ittisanronnachai, H. Itoi, L.-X. Li, K. Suzuki, U. Nagashima, H. Ogawa, T. Kyotani, M. Ito, Experimental and Theoretical Studies of Hydrogen/Deuterium Spillover on Pt-Loaded Zeolite-Templated Carbon, J. Phys. Chem. C, 118 (2014) 9551-9559. https://doi.org/10.1021/jp5016802

[36] K. Mori, T. Fujita, H. Yamashita, Boosting the activity of PdAg alloy nanoparticles during H_2 production from formic acid induced by CrO_x as an inorganic interface modifier, EES Catal., 1 (2023) 84-93. http://dx.doi.org/10.1039/D2EY00049K

[37] T. Yoshii, K. Nakatsuka, T. Mizobuchi, Y. Kuwahara, H. Itoi, K. Mori, T. Kyotani, H. Yamashita, Effects of carbon support nanostructures on the reactivity of a Ru nanoparticle catalyst in a hydrogen transfer reaction, Org. Process Res. Dev., 22 (2018) 1580-1585. https://doi.org/10.1021/acs.oprd.8b00207

[38] Y.-J. Chou, H.-C. Ku, C.-C. Chien, C. Hu, W.-Y. Yu, Palladium nanoparticles supported on nanosheet-like graphitic carbon nitride for catalytic transfer hydrogenation reaction, Catal. Sci. Tech., 10 (2020) 7883-7893. http://dx.doi.org/10.1039/D0CY01703E

[39] C.C. Truong, D.K. Mishra, Y.-W. Suh, Recent catalytic advances on the sustainable production of primary furanic amines from the one-pot reductive amination of 5-hydroxymethylfurfural, ChemSusChem, 16 (2023) e202201846. https://chemistry-europe.onlinelibrary.wiley.com/doi/abs/10.1002/cssc.202201846

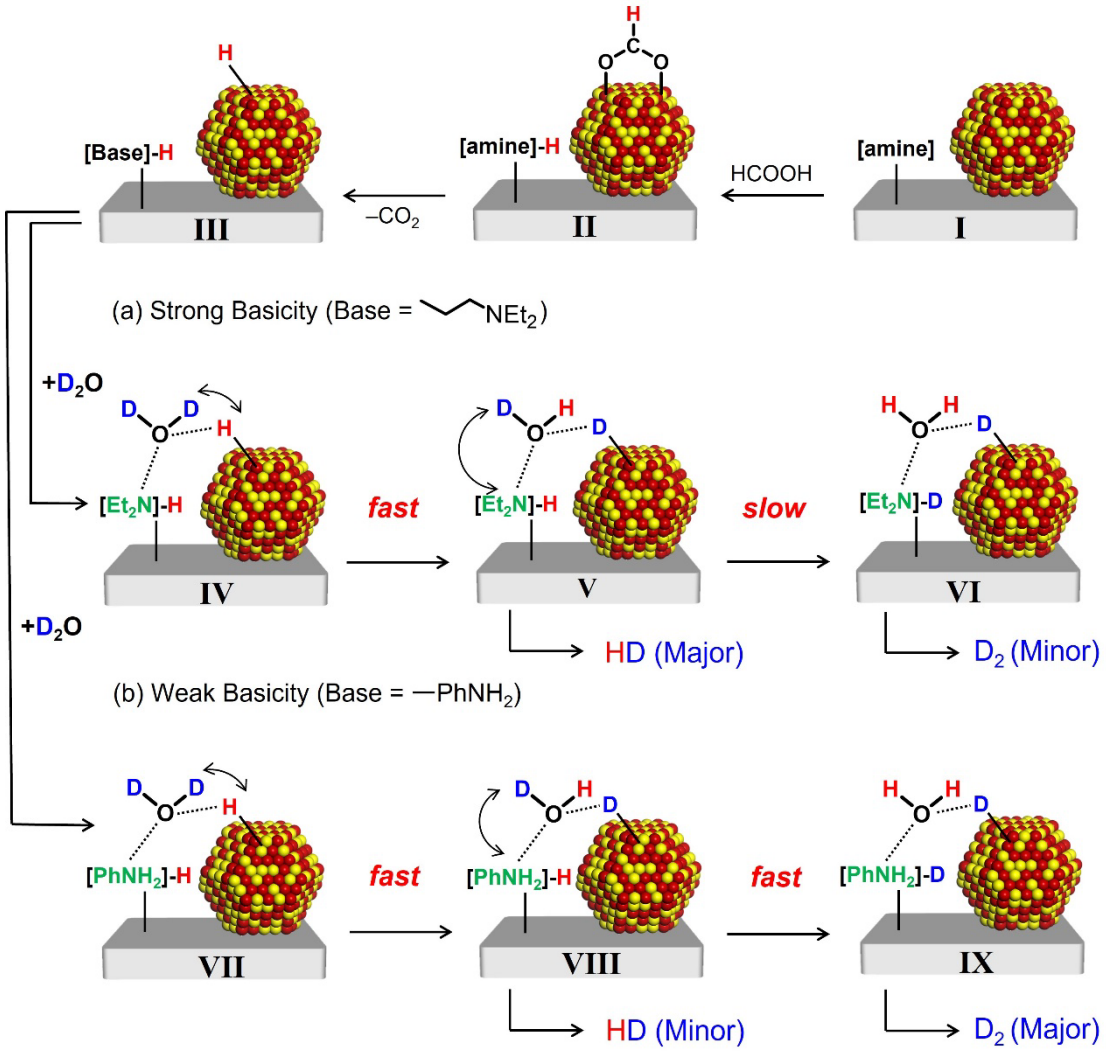

Figure 1. A proposed reaction mechanism for the selective release of hydrogen isotope gases (D_2 and HD) during the FA dehydrogenation in D_2O using a PdAg catalyst in the presence of (a) strongly and (b) weakly basic amine groups. The activation energy (E_a, in eV) is provided for each elementary step.

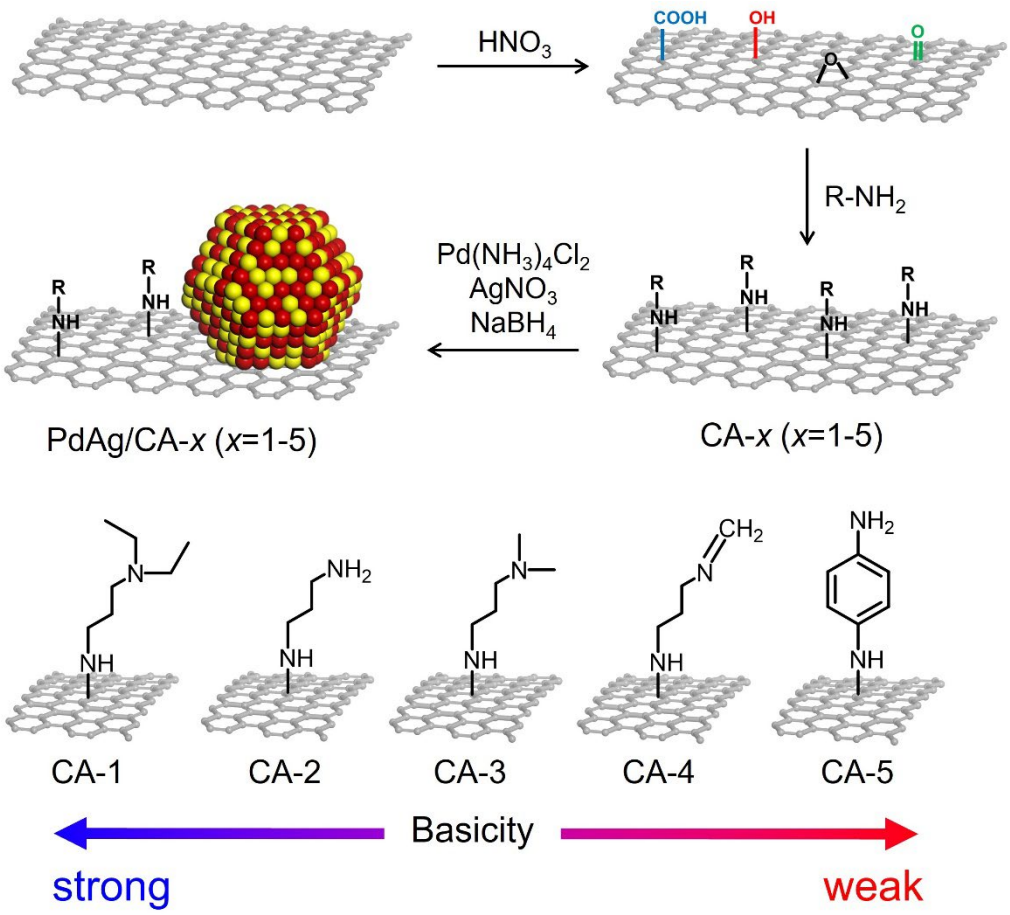

Figure 2. Illustrations summarizing the synthetic procedure used to produce a series of PdAg/CA-*x* (*x* = 1-5) specimens.

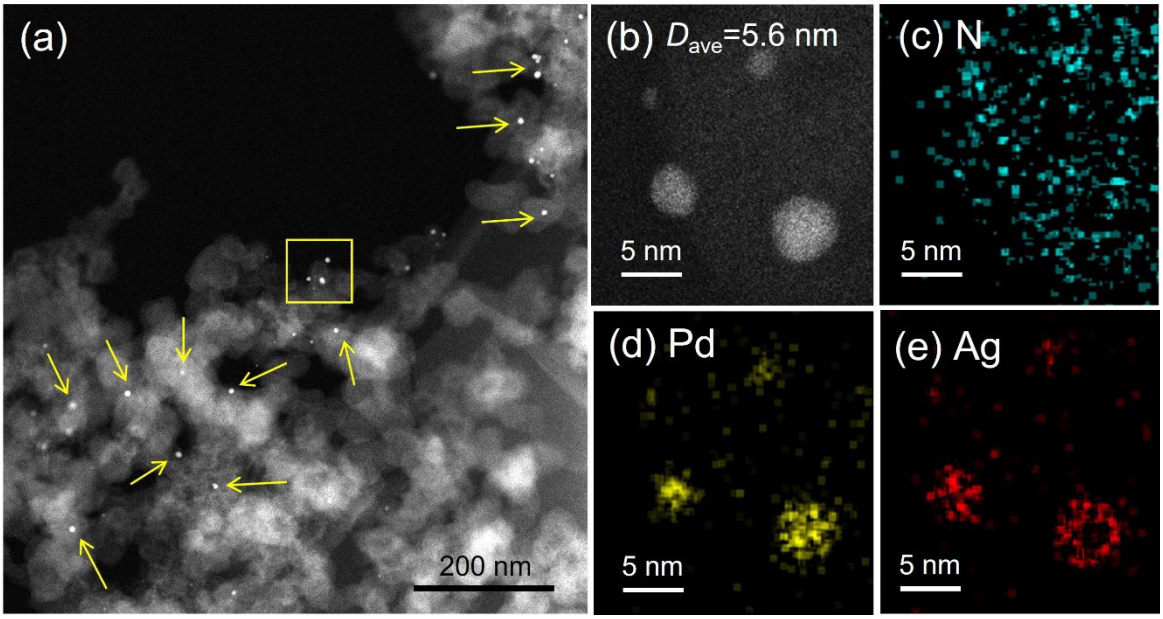

Figure 3. (a) A HAADF-STEM image of the PdAg/CA-5 and (b) a STEM image of the area indicated by the yellow square in (a). EDX maps of (c) Nitrogen (N), (d) Palladium (Pd), and (e) Silver (Ag) over the region shown in (b). The yellow arrows in (a) means the PdAg NPs.

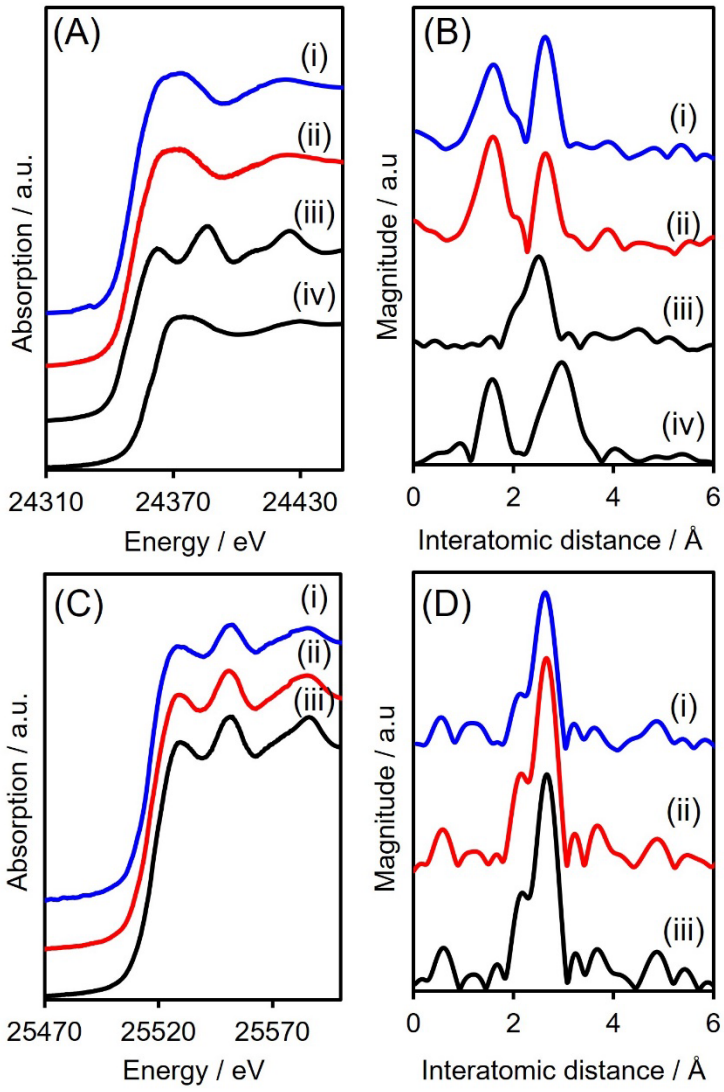

Figure 4. (A) Pd K-edge XANES and (B) EXAFS spectra obtained from (i) PdAg/CA-5, (ii) PdAg/CA-1, (iii) Pd foil, and (iv) PdO. (C) Ag K-edge XANES and (D) EXAFS spectra obtained from (i) PdAg/CA-5, (ii) PdAg/CA-1, and (iii) Ag foil.

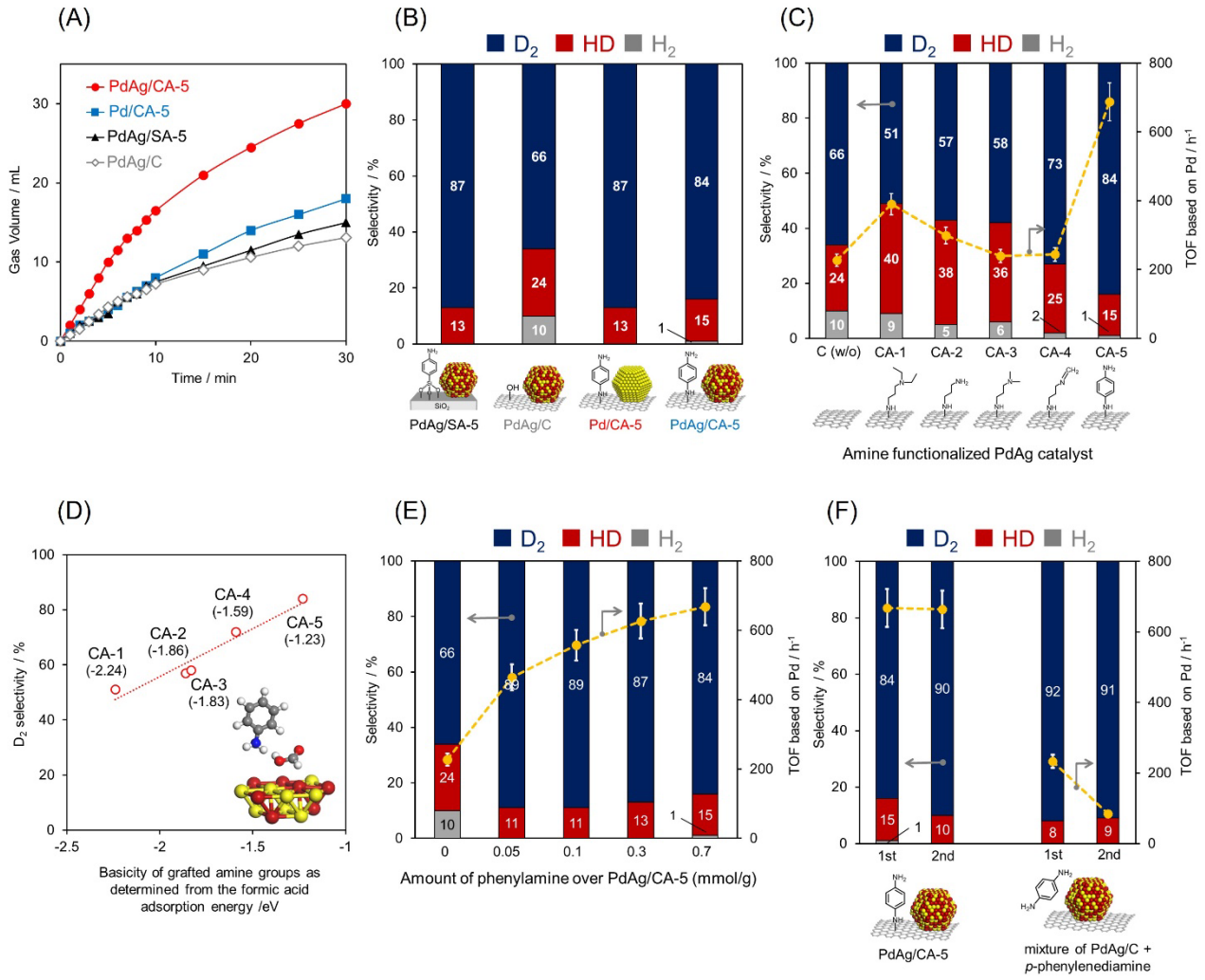

Figure 5. (A) Time courses of FA dehydrogenation reactions in D_2O at 343 K for 30 min. (B) Effects of alloying and amine functional groups on hydrogen isotope selectivity. (C) Hydrogen isotope selectivity obtained by PdAg/C and PdAg/CA-*x* (*x* = 1-5) in D_2O at 343 K for 30 min, and TOF values based on Pd. (D) Correlation between D_2 selectivity and basicity of amine group as calculated by E_{ad} of FA. (E) Effects of the amount of phenylamine on hydrogen isotope selectivity and TOF values based on Pd using the PdAg/CA-5 in D_2O at 343 K for 30 min. (F) Hydrogen isotope selectivity and TOF values based on Pd during recycling experiments with PdAg/CA-5 and a physical mixture of PdAg/C and *p*-phenylenediamine.

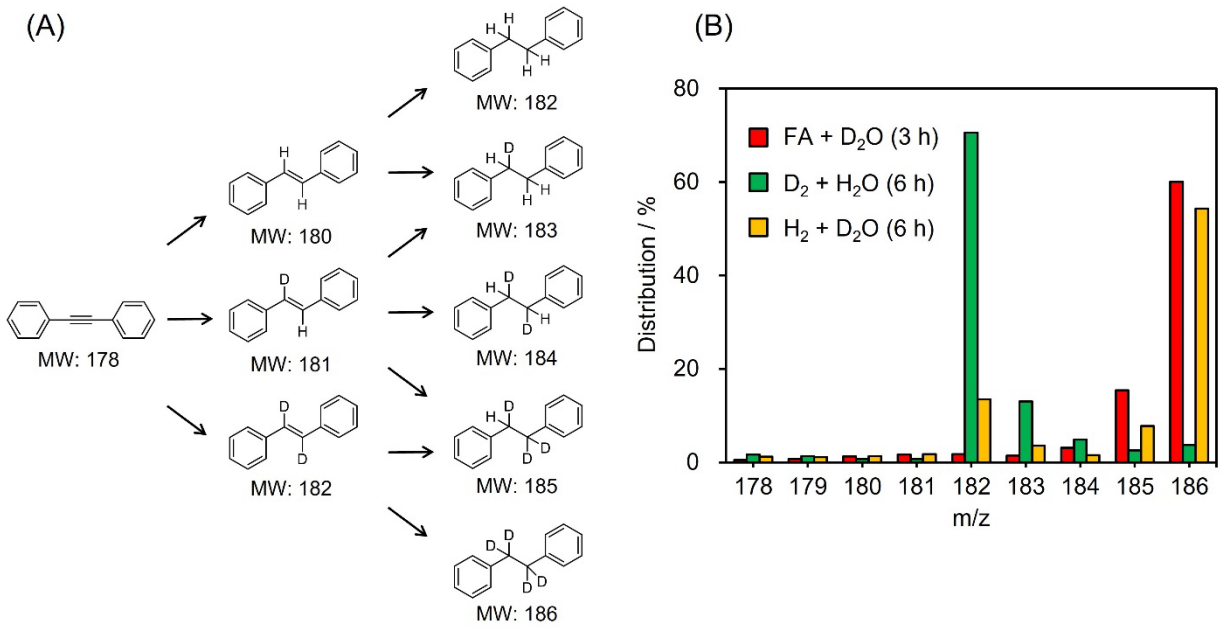

Figure 6. (A) Possible deuterated diphenylacetylene compounds and corresponding molecular weight (MW) values. (B) The product distribution as demonstrated by the intensity of ion peaks at various m/z. Data were acquired by gas chromatography/mass spectrometry following the *in situ* deuteration of diphenylacetylene in the presence of PdAg/CA-5 for 3 h.